

Reducing the Hydraulic Resistance in the Inlet Device of the Gas Turbine Unit

Oleg Baturin, Daria Kolmakova^a, Grigorii Popov^b, Vasilii Zubanov^c
and Yulia Novikova

Samara National Research University, Samara, Russia

Keywords: Hydraulic Losses, Work Shaft, Gas Pumping Unit, Inlet Unit.

Abstract: The paper presents the results of numerical simulation of air flow through a modernized variant of the inlet filter unit (IFU) of the gas compressor unit GPA-Ts-16. A feature of the IFU design is that to reduce the load on the filter unit, it is proposed to be as compact as possible, which determines its complex shape. The goal of the study is to study the hydraulic losses and to develop the measures to reduce them, since it is found that every 100 Pa of losses in the inlet unit increases the consumption of fuel gas by 2.5 kg/h or reduces the engine power by 10.5 kW. Calculations of hydraulic losses in IFU are carried out for cases of absence or presence of wind with a velocity from 0 to 35 m/s, blowing from 5 main directions (0°, 45°, 90°, 135°, 180°). Studies are also carried out on the effect of the weather shield shape, presence of baffles under it, and the rack in the shaft on the hydraulic losses. As a result of the research, recommendations are provided for designing (changing the shape) of the inlet filter unit that eventually allow to propose a design that will reduce the hydraulic losses in IFU by 15% relative to the originally suggested variant.

NOMENCLATURE

DIS – de-icing system;
FB – filter box;
GPU- gas pumping unit;
GTU – gas turbine unit;
IFU – inlet filter unit;
PJSC - Public Joint Stock Company;
SAC – Standard Atmospheric Conditions;
 Δp – pressure drop, Pa;
T – temperature, K.


1 INTRODUCTION


The Russian Public Joint Stock Company Gazprom today is one of the largest energy companies in the world. Its main activities are geological exploration, production, transportation, storage and sale of gas, gas condensate and oil, as well as the production and sale of electricity and heat. PJSC Gazprom provides


a continuous cycle of gas supply from the field to the consumer (Gazprom, 2019; Zabelin et al., 2013).

The peculiarity of the gas industry of the Russian Federation is that its main gas fields are located to the east of the Urals, and gas consumers are in Europe and China. Such a geographical location determines the presence of a large and extensive gas transmission system, through which natural gas is supplied from the field to the consumer. For example, the length of the Druzhba gas pipeline (across the territory of the former USSR) is approximately 3,900 km, and of the Soyuz gas pipeline is 2,750 km (Druzhba pipeline, 2019) (Figure 1). In total, PJSC Gazprom owns 161.7 thousand km of trunk pipelines included in the unified gas supply system of Russia (Zabelin et al., 2013).

An important element of any gas transportation system is gas pumping stations, which increase the pressure of natural gas in the gas pipeline and give an impulse necessary for its movement. Compressor stations are located evenly along the entire pipeline every 100...150 km. In 2013, PJSC Gazprom had 215 linear compressor stations, 6 gas processing

^a  <https://orcid.org/0000-0003-2806-3073>

^b  <https://orcid.org/0000-0003-4491-1845>

^c  <https://orcid.org/0000-0003-0737-3048>

complexes and 25 underground gas storage facilities, also using compressor stations. 87.2% of compressor stations have a gas turbine drive (about 3400 gas turbine engines (GTE) in total) (Zabelin et al., 2013).

Among the GTUs owned by PJSC Gazprom, over 18% are NK-16ST engines (Figure 2) with a capacity of 16 MW, developed at PJSC Kuznetsov (Zabelin et al., 2013; JSC "Kuznetsov", 2019) in the late 1970s based on the NK-8 aviation engine and operating as part of GPA-Ts-16 (Figure 3).

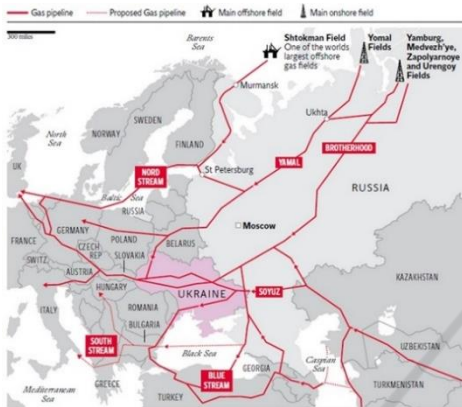
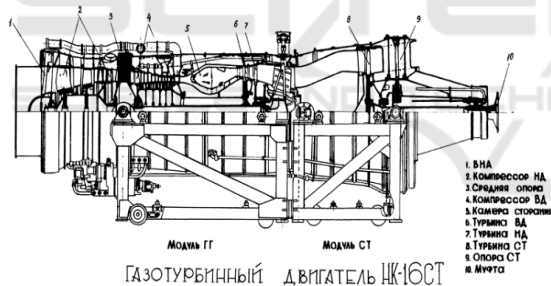


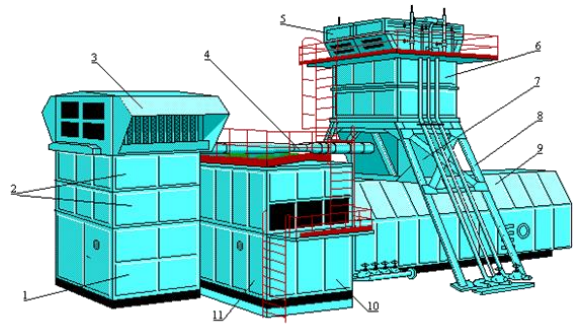
Figure 1: Gas transportation system of Russian (INNOVAES, 2019).



1 - Inlet guide vane; 2 - Low pressure compressor; 3 - Middle annular frame; 4 - High pressure compressor; 5 - Combustion chamber; 6 - High pressure turbine; 7 - Low pressure turbine; 8 - Free turbine; 9 - Free turbine bearing; 10 - Clutch.

Figure 2: Gas turbine drive of gas compressor unit NK-16ST (RTEH GTD NK-16ST Vse o transporte gaza, 2019).

GPA-Ts-16 showed good performance and high reliability. For this reason, a significant part of GPUs that have been overaged is not replaced with modern ones, but is being repaired, combining the replacement of outdated units with modernization aimed at reducing costs (increasing efficiency) and eliminating deficiencies identified in operation. During modernization, baseline unit has low level of filtration and quickly clogs up in snowy weather.



1 - turning part of the inlet shaft; 2 - inlet sound absorber; 3 - air cleaning device; 4 - cyclic air heating system; 5 - heat recovery; 6 - exhaust sound absorbers; 7 - diffuser; 8 - exhaust support; 9 - engine compartment, 10 - oil system units

Figure 3: Gas pumping unit GPA-Ts-16 (RTEH GTD NK-16ST Vse o transporte gaza, 2019).

2 RESEARCH OBJECT

The inlet filter unit of an industrial gas turbine is intended for cleaning cyclic air coming from the atmosphere to the engine inlet from dust and other mechanical inclusions at all possible modes of operation. IFU, despite its apparent simplicity (compared to the engine), is an important element of the GPU, in which complex processes take place. IFU must reliably clean the air entering the gas turbine unit from impurities to avoid critical damage to the elements of the flowing part by foreign objects. In this case, the pressure losses must be minimal to improve the efficiency of the engine and prevent compressor surge. The inlet unit must exclude clogging of filter elements with snow and ice at all operating conditions. Errors in the creation of IFU can significantly reduce the operational properties of the entire gas turbine station, however, this component is usually referred to the secondary elements of the engine and less attention is paid to its perfection than, for example, to the compressor.

One of the companies engaged in the supply of equipment for the GPA-Ts-16 under modernization is LLC Volga-Energogaz, which office is in Samara (Russia) (VolgaEnergogaz, 2019). The engineers of this company offered several variants of the IFU of GPA-Ts-16 and appealed to the Department of Aircraft Engine Theory (Department of Aircraft Engine Theory, 2019) of the Samara National Research University (Samara University, 2019) with a request to evaluate the level of hydraulic losses in IFU variants, and to help in choosing the final variant.

The IFU design proposed by LLC Volga-Energogaz consists of a weather shield with an inlet from the bottom, a filter box with two-stage Folter cassette filters with filtration class G4/F8 (Air inlet Filtration for GAS turbines, 2019), a diffuser, a vertical shaft with sound absorbing panels, a turning channel, an engine inlet duct with lemniscate and de-icing system pipelines (Figures 4 and 9). The proposed IFU variants differed in the shape of the weather shield (with straight walls and roundings) and the presence/absence of baffles in the inlet section below it and a rounded rack in the turning channel.

The vertical shaft, the turning channel and the engine inlet duct with lemniscate are adopted from the existing GPA-Ts-16 mine. The remaining elements are being developed and will be manufactured again.

The main idea of the modernization is the replacement of the inertial filters which proved to be unsatisfactory with the two-stage Folter cassette filter with the filtration class G4/F8 of the square shape with dimensions of 592x592mm. A clean filter of this type has a hydraulic resistance of 75 Pa. The maximum pressure drop on the contaminated filter reaches, according to the manufacturer, 450 Pa (Air inlet Filtration for GAS turbines, 2019). Unfortunately, more detailed filter permeability characteristics are not known.

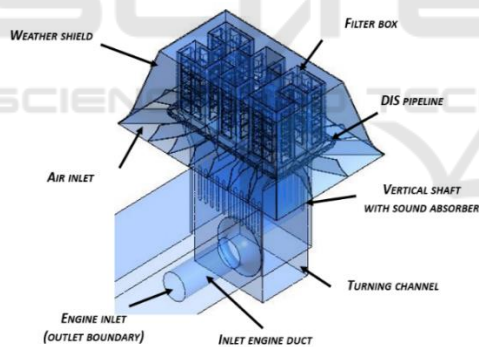


Figure 4: Proposed IFU design.

The required number of filters (124 pieces) is selected based on the nominal air flow rate through the engine 102 kg/s, considering 15% of the reserve (i.e. based on the mass flow rate of 117 kg/s). In the baseline variant, it is assumed that there are 4 filters along the height of the filter box. This required to increase the lateral area of the filter box for their placement by the increasing complexity of its shape (Figures 4 and 5), considering the required number of filters. In this case, the designers seek to keep the minimum size of the filter box to reduce the load on the shaft.

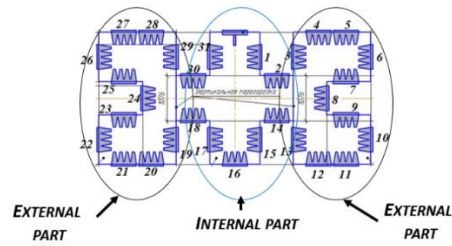


Figure 5: The adopted shape of the filter box (in plane) with their accepted numbering.

3 THE INFLUENCE OF HYDRAULIC LOSSES IN THE INLET UNIT ON THE EFFICIENCY OF THE ENGINE GPU

At the first stage, using the thermodynamic model of the NK-16ST engine, created and verified according to the data provided by PJSC "Kuznetsov" (JSC "Kuznetsov", 2019), a study of the influence of the hydraulic perfection of the IFU of this engine on the fuel consumption in the case of maintaining a constant power of 16 MW (Figure 6) is conducted. A study on the effect of hydraulic perfection of IFU on engine power at a constant flow rate of fuel gas is also carried out (Figure 7).

The results show that an increase in hydraulic losses in IFU leads to a linear increase in fuel gas consumption and a decrease in power. Every 100 Pa of losses in the inlet unit increases the fuel gas consumption by 2.5 kg/h or reduces the engine power by 10.5 kW.

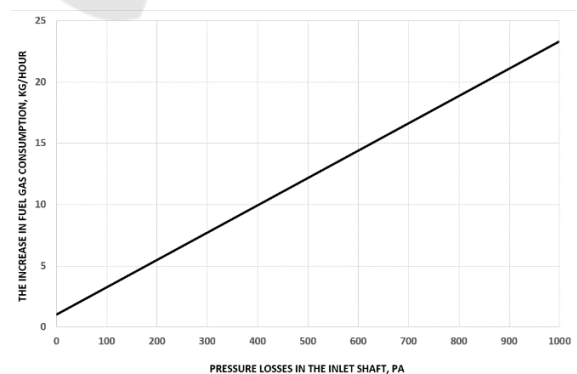


Figure 6: The increase in fuel gas consumption of the NK-16ST depending on the hydraulic losses in the inlet unit under the constant power.

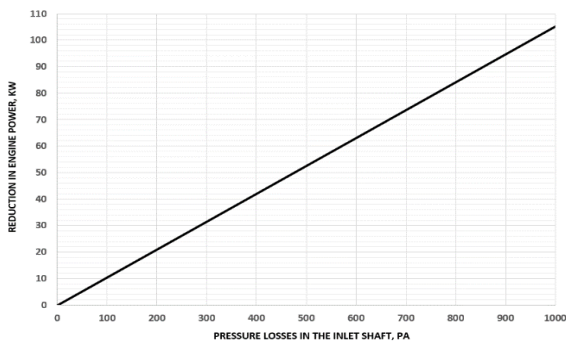


Figure 7: Decrease in the power of the NK-16ST depending on the hydraulic losses in the inlet unit at a constant consumption of fuel gas.

4 DESCRIPTION OF COMPUTATIONAL MODEL

The design model for determining the hydraulic losses in IFU of GPA-Ts-16 is created in the NX and Ansys CFX software in accordance with the drawings provided by LLC Volga-Energogaz.

The computational model includes a part of the atmosphere around the inlet shaft and a flowing part of the IFU with an engine block simulator (Figure 8). The modeling of the surrounding atmosphere is necessary to correctly simulate the fields of parameters at the inlet to the shaft, considering changes in the direction and velocity (force) of the wind. The engine block simulator is used to consider the effect of gas pumping unit blocks in modeling winds blowing from the engine side. The model considers the full geometry of the channels, the presence of filters, sound absorbing panels, racks in the transition duct (if available), pressure drop in the filter elements, ring collector of DIS, etc. The presence of the operating floor around the perimeter of the filters is not considered. Filters are modeled simplified (see below).

In the numerical simulation of the working process in the inlet shaft, the following boundary conditions are applied:

- The inlet condition is applied at the boundary of the considered part of the atmosphere. The air temperature (in SAC) $T_a = 288$ K, the velocity (in m/s) and the direction of the wind (as direction cosines) are set for it. In all cases, it is assumed that the wind blows parallel to the surface of the earth.
- The outlet boundary of the model is located at the engine inlet. The mass flow rate through the engine is set for it.

- The surface of the earth is an impenetrable wall. For the calculation, it is assumed that during the "numerical experiment" the engine operational mode (mass flow through it) and atmospheric pressure do not change. It is also assumed that the mass flow rate of air through the engine is identical for all considered working conditions. In other words, the response of the GTE control system to weather conditions is not taken into account.

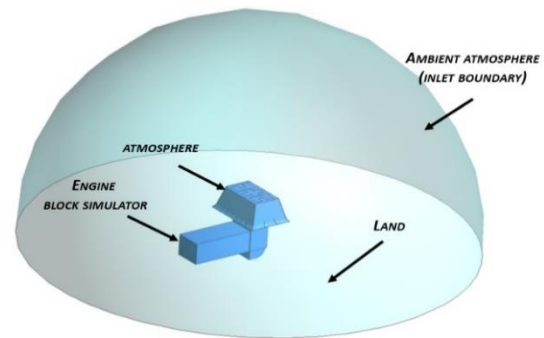


Figure 8: Computational model of the inlet shaft of the GPA-Ts-16.

Because the exact geometry and permeability characteristics of the filter materials are not known, they are modeled as follows. The filter geometry is simplified, and its shape is parallelepiped. A condition (interface) is imposed on it according to which the flow falling on the inlet surface 1 is transferred to the outlet surface 2 in such a way that the pressure on the surface 2 is less than 1 by the amount of pressure drop in the filter Δp . Thus, in the created computational model, total pressure losses on the filters are considered the same in all filters (the filters are uniformly polluted), regardless of external conditions (wind speed and direction).

An ideal gas with air properties and variable heat capacity and viscosity is used as a working fluid in the simulation. When calculating, the turbulence model $k-\epsilon$ with a scalable wall function is used in calculation.

The calculation model is meshed by a finite volume grid (Figure 9). It is based on tetrahedral elements in combination with a prismatic layer on the surface of streamlined walls. The total number of final volumes is 11 million. The number of finite volumes is selected based on the study of mesh convergence, the results of which are shown in Table 1. In the course of the study, 4 models were created based on one computational model corresponding to the initial geometry (Variant 1, Table 2), differing in the density of the finite volume mesh.

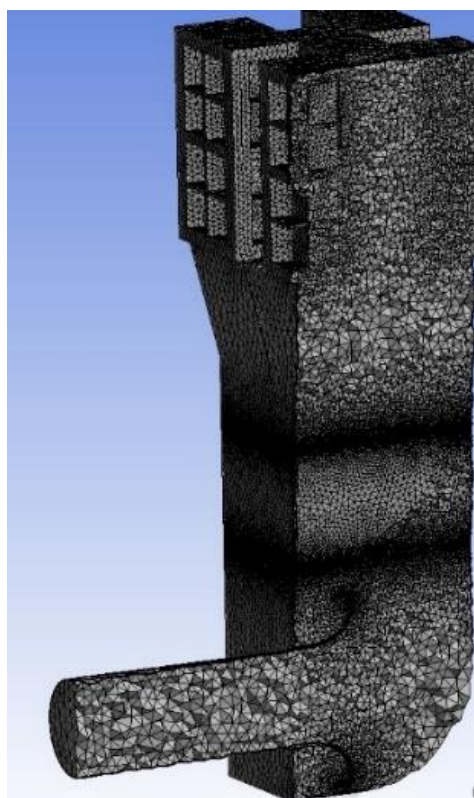


Figure 9: The grid of finite volumes of the created computational model.

Table 1: Results of the study of the mesh convergence of the computational model.

The number of model elements, mln	2	5	11	39
The drop in total pressure in the shaft, Pa	703	728	750	746

It is obvious from Table 1 that the global numerical values obtained by models with a mesh of 11 and 39 million elements are close, but the computation time in the latter case is significantly higher. Therefore, in the future, a mesh with an approximate number of elements of 10...12 million is adopted for all studies (the number of elements changed due to changes in the geometry of the shaft).

Due to the large dimension of the computational grid, gas-dynamic modeling is carried out on the “Sergey Korolev” supercomputer (Supercomputer Center - Samara University, 2019). The calculations involved 128 cores and 128 GB of RAM.

During the study, 4 variants of the inlet shaft design (Table 2) are considered:

- Variant 1 - In accordance with the drawing provided by the Customer (Figure 11) (with roundings and baffles at the inlet and rack in the turning channel);
- Variant 2 - Option without rounding and baffles, but with a rack;
- Variant 3 - Identical to Variant 1, but without a rack (Figure 4);
- Variant 4 - Identical to Variant 1, but without baffles.

Table 2: Scheme of differences of the considered variants.

Variant	1	2	3	4
Rounding at the inlet of the weather shield	+	-	+	+
Baffles at the inlet	+	-	+	-
Rack in the turning channel	+	+	-	+

All variants are considered in the absence of wind and in the presence of winds at velocity of 10, 20 and 35 m/s from five main directions (0°, 45°, 90°, 135°, 180°) (Figure 10).

To simplify the analysis of the obtained results, the averaged values of the flow parameters and contours of the parameters (velocity and pressure) in the flowing part are considered in 7 control sections along the path (Figure 11):

- 0 - the lower edge of the weather shield (is absent in variant 2);
- 1 - lower edge of weather shield after baffles;
- 2 - at the inlet to the filters (box-shaped);
- 3 - between filter box and diffuser;
- 4 - in front of sound absorbing panels;
- 5 - after sound absorbing panels;
- 6 - at the GTE inlet.

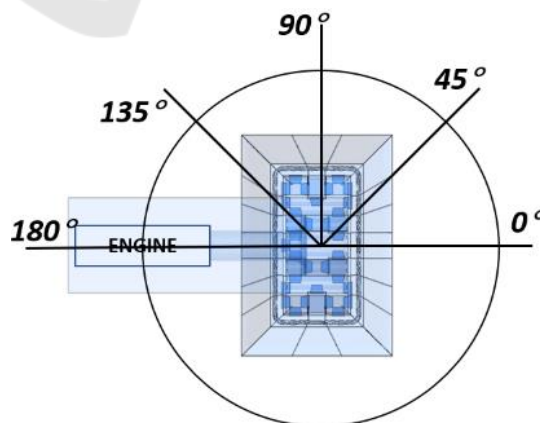


Figure 10: Main wind direction.

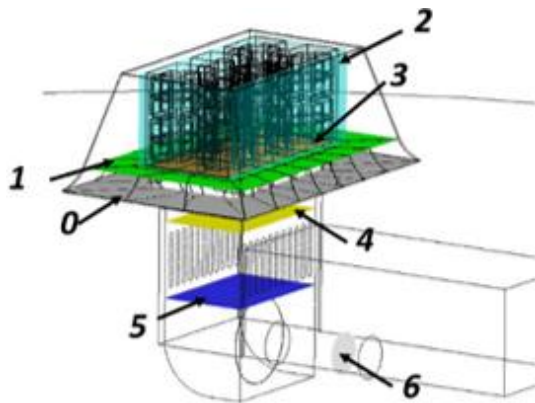


Figure 11: Considered IFU control sections.

5 STUDY OF THE IFU WORKFLOW IN CALM WEATHER

Summarized data on the expected values of total pressure losses in the considered IFU variants without the wind effect (wind velocity is 0 m/s) is shown in Figure 12. Losses are calculated as an algebraic difference between the area-averaged values of the total pressure in the control sections. The distribution of total pressure losses between the section of the IFU flowing path for the considered variants without wind is shown in Figure 13.

It is clear from the figures that all the considered variants show close hydraulic characteristics (total pressure losses) in calm weather. The difference between the four variants is no more than 30 Pa. In calm weather, the total pressure losses vary from 380 (with clean filters) to 750 Pa (with dirty filters).

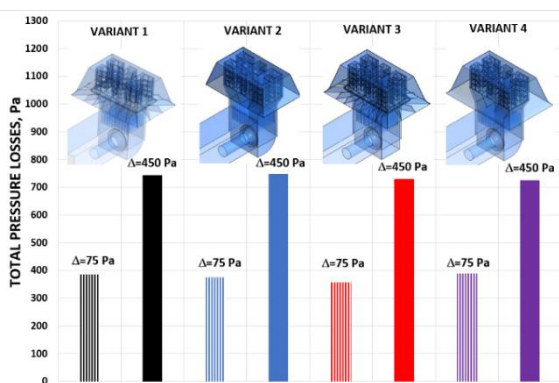


Figure 12: Total pressure losses in IFU for various modifications of the baseline design in calm weather.

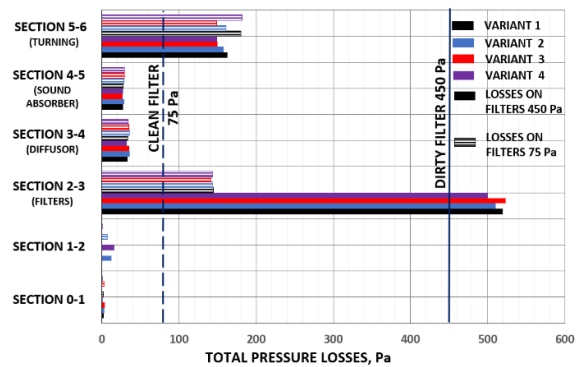


Figure 13: Total pressure losses in IFU elements for various modifications of the baseline design in calm weather.

The total hydraulic losses in the flowing part of IFU in calm weather for all the considered variants do not differ and are approximately 310 Pa (excluding losses in the filters).

As can be seen from the obtained results, the physical picture that occurs with “clean” ($\Delta p = 75$ Pa) and “dirty” ($\Delta p = 450$ Pa) filters is identical under the assumptions made (uniform contamination of filters). The difference is only a quantitative estimation of the hydraulic losses (the computational models for estimating losses with clean and dirty filters are identical, except for the pressure drop at the interfaces simulating the operation of the filter (75 Pa for clean filter and 450 Pa for dirty filter).

For this reason, in the future, all computational models are calculated only with “dirty” filters ($\Delta p = 450$ Pa), since this option is the ultimate in terms of losses.

The main losses of total pressure in the shaft occur when the working fluid passes through the filters (section 2-3) and when the flow turns in the transition duct and moves in the channel before entering the engine (section 5-6). In the first two section (0-2) with zero wind, the loss of total pressure is negligible. Losses in the diffuser (section 3-4) and in sound absorbing panels (section 4-5) are relatively small (do not exceed 40 Pa) and do not depend on the shaft design.

It should be noted that the losses in the filter box are largely determined by the losses on the filter element. Additional losses in this component do not exceed 70 Pa.

The reason for the increased losses when turning the flow in the turning channel and in the inlet channel of the GTE is in the fact that during the flow of the working fluid, vortex zones appear on the right and on the left of the engine, as well as a high level of velocity (up to 70 m/s) in the engine inlet channel.

The vortex in the turning channel is generated as follows. The internal part of the filter box is divided by baffles into three parts (two external and one internal) (Figure 5). The air passing through the filters of the inner part is directed vertically downward directly to the engine inlet and is immediately sucked into it (Figure 14). Only a small part passes by and interacts with side vortices or falls into the space between the lemniscate and the front wall of the engine block.

At the same time, the air trapped in the outer parts, passes a more complex trajectory. For example, air passed through filter No. 6 (Figure 5) goes through all the space of the filter box almost to filter No. 3 (Figure 14) and turns down there. The air that has passed through the side filters No. 4, 5, 7 (Figure 5) interacts with the flow through filter No. 6 and almost immediately turns down. Thus, a substantial mass of the working fluid from filters No. 4-7 moves in the direction of the filter No. 3 (Figure 5) inside the box. As a result, the working fluid passes through the filter No. 3 only in the lower sections outside. From the upper sections, the working fluid is pulled out in the opposite direction (Figure 15). Thus, with the adopted configuration of the filter box, not all filters work in the same way. Filters facing the atmosphere pass the working fluid through only in the “inward” direction. Part of the filters located in the recesses (“pockets”), pass the working fluid in smaller quantities, or vice versa release it back.

In Figure 15 and further on similar graphs (Fig. 21 and 24), a circular diagram of the distribution of air flow between the vertical rows of filters is shown. This graph is plotted in the polar coordinate system. In it, along the radius, the total value of the mass flow rate through the vertical row of filters in kg/s is deposited. A positive sign indicates that the working fluid flows into the filter unit, a negative one indicates that it flows out. The angular position corresponds to the number of the filter row according to Figure 5 (indicated on the periphery of the circle).

Figure 15 illustrates this fact, showing the distribution of working fluid mass flow rates between the vertical rows of filters for all 4 considered IFU variants (excluding wind) with maximum and minimum pressure losses on the filters. Thus, in calm weather, 4 vertical rows of filters do not work (the working fluid flows out of them) and another 4 rows work with reduced flow rates.

Analysis of the flow structure (Figure 16) of the considered IFU variants shows that in calm weather, air enters the shaft from all directions, uniformly filling the entire inlet section.

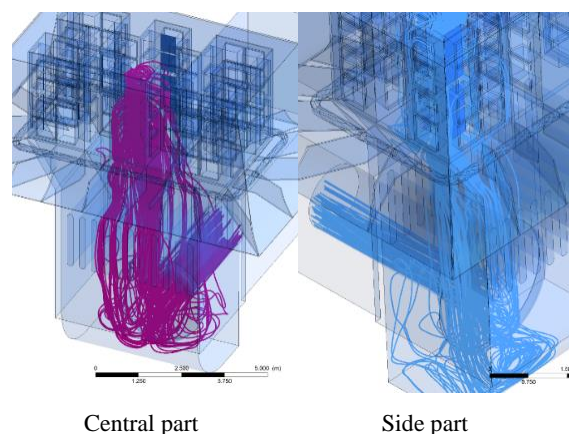


Figure 14: An example of the flow of air through the various sections of the filter box.

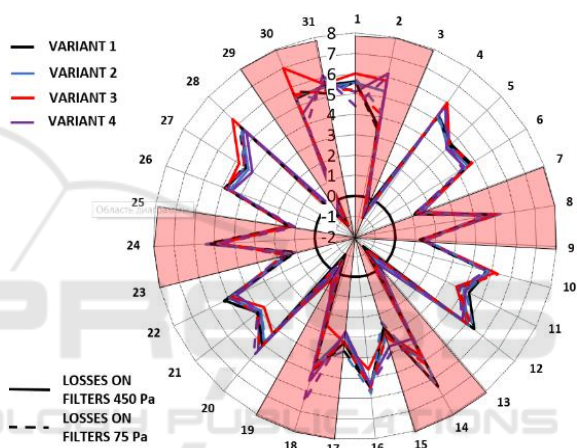


Figure 15: The distribution of the flow rates of the working fluid between the filters (the numbers correspond to Figure 5) (the shaded areas correspond to the filters in the “pockets”).

If we compare the flow structure in the variants without rounding of the weather shield walls (Variant 2) and with it (Variant4), it can be concluded that a large flow separation is formed on the inlet edge of the weather shield for the variant without rounding, which reduces the effective flow area, and increases the flow rate at the inlet to the filters. Thus, the rounding at the inlet to the weather shield forms a more favorable flow structure at the inlet, reducing the velocity at the inlet and its unevenness. In general, the rounding of the weather shield in calm weather reduces hydraulic losses by a relatively small value. However, in the presence of wind, the gain significantly increases.

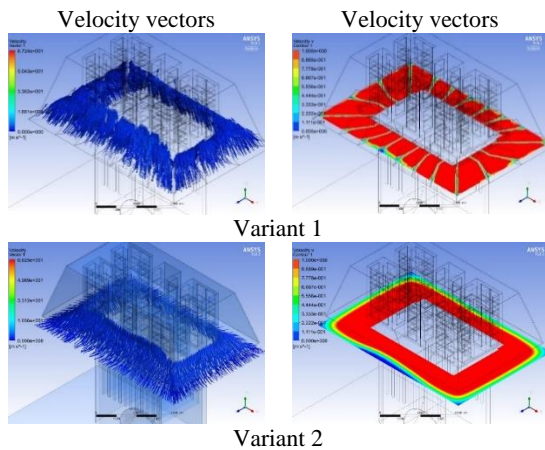


Figure 16: The flow structure in section 0 (inlet to the weather shield) for variant 1 and 2.

6 STUDY OF THE IFU WORKFLOW IN THE PRESENCE OF WIND

To assess the influence of wind force and direction on the working process and hydraulic losses of the inlet shaft, a study is conducted in which the wind velocity varies from 0 to 35 m/s and the direction from 0° to 180° (Figure 10).

Figure 17 shows how the values of the total pressure losses change in all the considered variants of the inlet shaft when the force and direction of the wind change. As can be seen, with increasing wind velocity, the hydraulic resistance of the shaft is constantly increasing. The increase in losses is not linear. With the wind velocity of up to 10...15 m/s, the losses of total pressure in the inlet shaft differ little from non-wind conditions. A further increase in wind velocity leads to an avalanche-like increase in losses.

In order to understand the causes of losses, the averaged (among all the calculated variants of the design and wind direction) total pressure loss values in characteristic sections of the inlet shaft at various wind velocities (Figure 18) are calculated.

The most intensive growth of losses is observed at the inlet to the shaft (section 0-2, more than 500 times with a change in wind speed from 0 to 35 m/s) and in filter box (by 70%). In the turning channel (sections 5-6), the growth of losses is moderate (30%). The greatest losses occur with side winds (45...135°). It is curious to note that the change in wind velocity and its force has little effect on the losses of total pressure in the diffuser and sound absorbing panels, which confirms the conclusion made earlier that minor

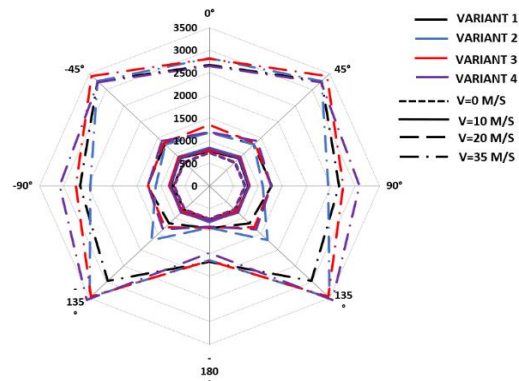


Figure 17: The dependence of the total losses of total pressure in the inlet shaft with different force and direction of the wind.

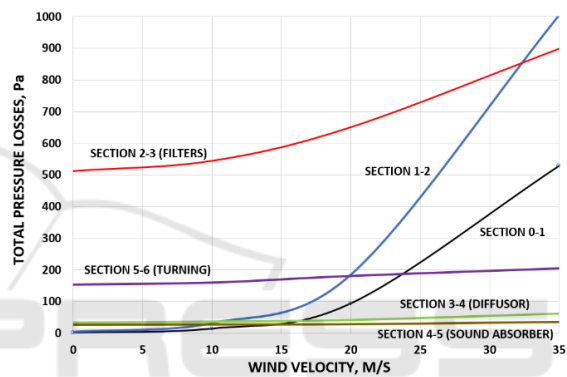


Figure 18: The change in the averaged values of the total pressure losses in the characteristic sections of the inlet shaft with increasing wind velocity.

design changes in these parts are not able to significantly change the shaft hydraulics.

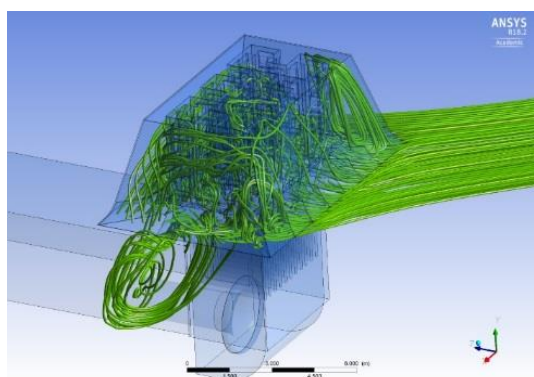
Some changes in the total pressure losses in the turning channel (section 5-6) is associated with a change in the flow structure there. In the presence of wind, there is a redistribution of air flow between the outer and inner parts of the filter box. The flow rate of the working fluid through the windward outer part increases, through the inner and leeward outer part - decreases. As a result, the intensity of the vortices and the average level of the flow velocity located on the right and left of the engine inlet change, the flow loses a symmetrical character, local flow accelerations appear (including in the filter box and sound absorber), the interaction of the vortices changes, which increases losses.

Losses in the section before the filters are associated with the formation of vorticity during flowing past the weather shield inside and outside. Figure 19 shows the trajectories of air particles before they fall under the weather shield when the wind direction is 45°. With other wind directions, the flow

structure does not change in principle. It can be seen that the working fluid is sucked into the shaft evenly from all directions in windless weather, but in the presence of wind the main part of the air enters from the narrow sector on the windward side. At the same time, when flowing the weather shield and shaft, a vortex structure is formed on the leeward side (Figure 19, 20).

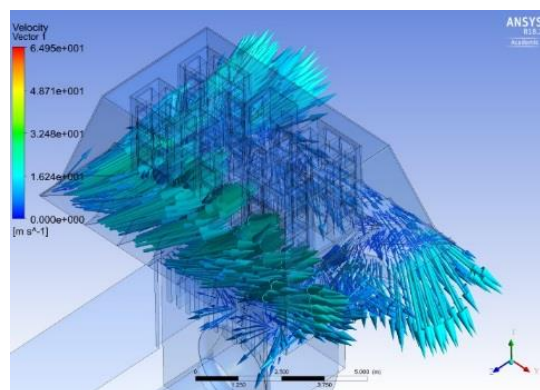
In calm weather, all the working fluid goes into the filters after passing section 0 along the shortest path. Overflow under the shield is minimal. In the presence of wind, the working fluid immediately enters the filters only on the windward side. At the same time, the air flow velocity increases substantially compared to calm conditions. The amount of working fluid that passes under the shield from the windward side is greater than the filters can pass through on this side, and the working fluid begins to flow to the leeward side. This overflow, coupled with areas of reduced pressure on the leeward side, caused by vortexes formation in the external flowing past the shaft, leads to a complex unsteady vortex structure between the inlet section and filter box inlet on the leeward side. These circumstances lead to the fact that the working fluid through the inlet section under the weather shield (section 0) enters unevenly, and there is a large number of backflows (Figure 20), which increases the values of local velocities there.

Another negative effect associated with such a flow pattern under the shield is that the DIS tubes installed in front of the filters is flowed not by air, which goes in the direction of the filters, but by a multidirectional and non-stationary flow. This will blur the field of increased temperature created by them and reduce the efficiency of the system.



Wind velocity - 20 m/s at an angle of 45°

Figure 19: The trajectory of the particles of the working fluid, before getting under the weather shield.



Wind velocity - 20 m/s at an angle of 135°

Figure 20: Flow velocity vectors in the inlet section of the shaft.

The described structure of the flow under the shield in the presence of wind leads to the fact that the distribution of flow rates between filter elements changes. To confirm this, Figure 21 shows how the mass flow rates of the working fluid change through filter groups at a wind direction of 0° at a wind velocity of 20 m/s. Distribution of mass flow rates for other wind directions is not fundamentally different.

As can be seen, the presence of wind has a significant impact on the distribution of mass flow rates between the filter sections. As a rule, on the windward side, the flow rate of working fluid through the filters increases. There is an increase of flow rate (at 20 m/s up to 3 times relative to windless weather) at the angles (90...135° and 220...270°) relative to the wind direction. In the presence of wind, the number of filter elements (by 4 pcs.) from which the working fluid is thrown back or the flow rate is significantly less than the average value (they are mainly concentrated in the “pockets” and on the leeward side) on average is 12, which is 1.5 times greater than in calm weather. The greatest number of filters that do not work properly takes place with side winds (45...135°).

The greatest pressure losses during the flowing past the weather shield occur when the wind blows into the corner (45° and 135°). This is because an additional vortex is generated under the shield from the inner side of the corner (Figure 22).

The presence of baffles streamlines the flow of the working fluid under the shield. Without baffles, the working fluid “hits” the lower row of filters, making the mass flow rate distribution between the filters of one vertical more uneven. On the windward sides, the working fluid also moves with a significant horizontal component, which adversely affects the operation of the DIS. The variant with rounding the lower part of

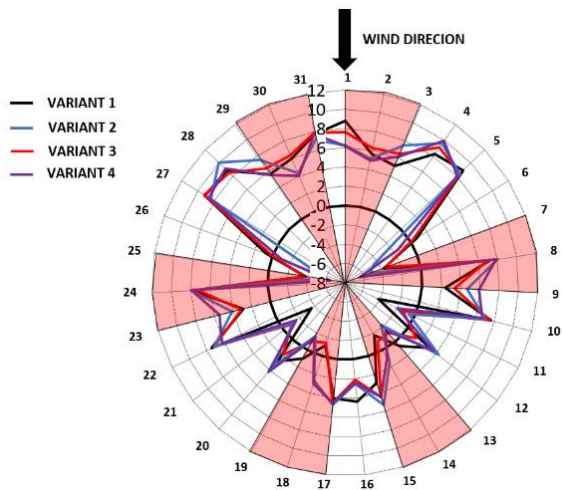


Figure 21: Distribution of mass flow rates through filters with a wind of 20 m/s, flowing at an angle of 0° (filter numbers correspond to Figure 13).

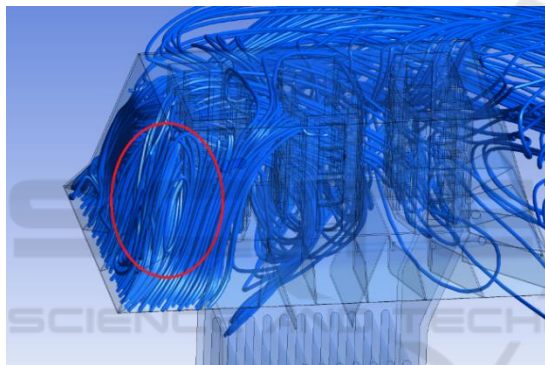


Figure 22: An additional vortex under the shield when the wind hits "into the corner" (the angle of 135°).

the weather shield, as in the case of windless weather, provides the best inlet under the weather shield, without additional vortex formation.

7 RECOMMENDATIONS FOR THE DESIGN CHANGE

As a result of the study, recommendations are made to change the baseline design of the IFU, which will reduce hydraulic losses:

- At the inlet to the space under the weather shield, it is necessary to install baffles, which will improve the performance of filters and PIC (especially if there is wind).
- For a more uniform entry of the working fluid and reduction of inlet losses, the weather shield must

have an extension at the inlet, but its design can be simplified.

- To reduce clutter on the inlet section, the DIS collector must be removed from section 0.
- Changes in the design of the diffuser and sound absorbing unit do not have a noticeable effect on the hydraulic perfection of the shaft.
- The presence of the rack in the turning channel does not affect the level of losses, and it can be removed from the design.
- The layout of the filters must be revised to reduce the number of abnormally operating filters. To reduce losses at side wind, it is necessary to increase the lateral projection of the filter box. In the ideal case, the filter box must have a square shape.
- To reduce the backflow from the filter unit inside it, it is necessary to install impermeable baffles.

8 INVESTIGATION OF LOSSES IN MODERNIZED IFU VARIANTS

Based on the recommendations given in the previous section, 2 variants of IFU are developed.

Variant 5 - In general, it is identical to Variant 3, but differs in the modified dimensions of the diffuser, filter box and weather shield, as well as in simplification of their shape (Figure 23).

Variant 6 - A variant which is characterized by a rectangular-shaped filter box (Figure 24, in which (8 (in width)*6 (in length)*5 (in height) filters are located), by the absence of sound absorbing panels and by a weather shield with additional windows in the side walls.

For both modernized variants, computational models are created, similar to those described above. The calculations show that Variant 5 has the hydraulic characteristics close to the Variant 3. The magnitude of the pressure loss increased by 40 Pa (5%).

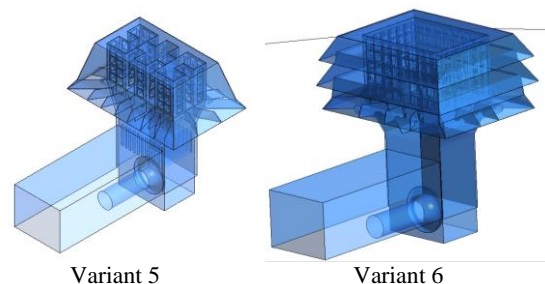


Figure 23: Modernized IFU variants.

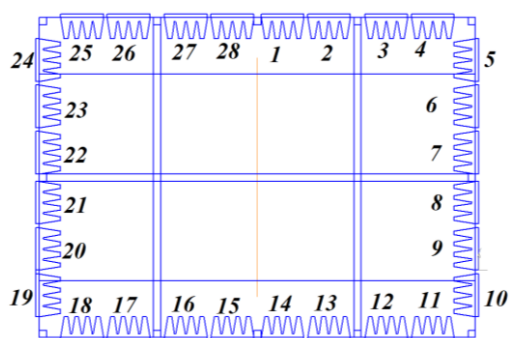


Figure 24: Adopted filter numbering in Variant 6 of IFU.

Variant 6 ensures the achievement of minimal losses among all the considered variants of IFU. In the absence of wind, the expected total hydraulic resistance in the upgraded IFU is: initial - 260 Pa (taking into account the resistance of clean filters of 75 Pa), final - 635 Pa (taking into account the resistance of dirty filters of 450 Pa). This is 107 Pa (15%) less than the baseline variant of the design (No. 1). The reason for the improvement is the absence of sound absorbing panels, a lower level of losses at the inlet and a greater uniformity of flow at the inlet to the filter elements.

The average velocity at the inlet to the filter box of the Variant 6 in calm weather is 1.78 m/s (for comparison, in the baseline design (No. 1) is 3.01 m/s), at the inlet to the weather shield is 1.52 m/s (for Variant 1 is 2.09 m/s). Note. The velocity of flowing on the filter element recommended by the filter manufacturer is less than 2.5 m/s.

In calm weather, the distribution of the flow rates of the working fluid through the vertical rows of filters of IFU No. 6 is close to uniform (4.25 ± 0.25 kg/s). In contrast to the previously considered variants, in IFU No. 6 under no-wind conditions there are no sections with a significantly different level of mass flow rates of the working fluid, or through which the working fluid flows out (Figure 25).

Variant 6 in windless weather provides a significantly more uniform "loading" of filters, which reduces the velocity level of air flowing on them. It should also be noted a smaller difference in the distribution of velocities (Figure 26) along the height of the filter box which suggests that Variant 6 provides large flow rates through the upper filters and, consequently, reducing flow rates through the lower ones. These facts indicate more favourable conditions for the operation of filter elements in Variant 6.

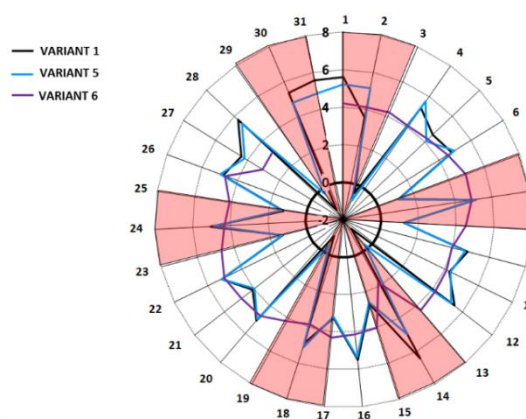


Figure 25: The distribution of the flow rates of the working fluid between the filters (numbers for variants 1-5 - Figure 5, variant 6 - Figure 23 (pink areas correspond to the filters in the "pockets" for variants 1-5).

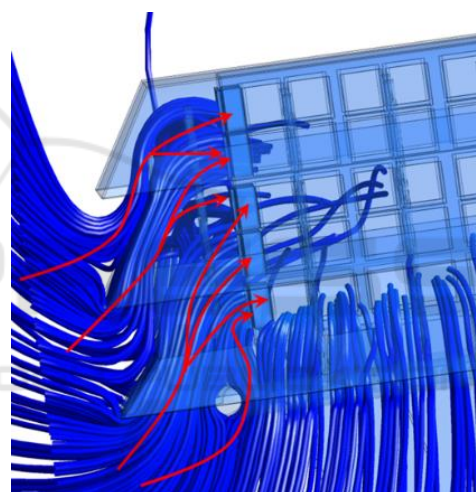


Figure 26: The flow structure through the entrance windows of the weather shield of the IFU No. 6 in calm weather.

In the presence of wind at 20 m/s, blowing strictly into the face of the shaft, Variant 6 exceeds the baseline variant (number 1) in hydraulic losses by ~150 Pa. With the direction of the wind "from an angle" (45° and 135°), the modernized variant shows a higher level of losses by 150 Pa. The reason for the increased losses in the characteristics of the air flow in the space between the weather shield and the filter box (Figure 27).

To reduce the intensity of vorticity and streamline the flow structure under the weather shield, its shape must be optimized, and internal baffles must be installed similar to the baffles near the lower edge of the weather shield. To select the shape and position of these baffles, considering the effect on the

complexity of the maintenance of IFU, additional research is necessary.

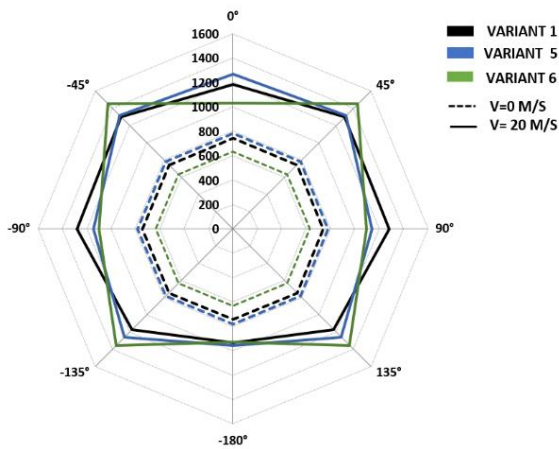


Figure 27: Dependence of the total loss of total pressure in IFU of the main variants of the inlet shaft at a wind of 20 m/s with its different direction.

9 CONCLUSIONS

In the current research, a numerical simulation is carried out of the air flowing in various variants of the modernized inlet unit of the GPA-Ts-16 gas-pumping unit with a two-stage cassette filter.

The values of total pressure losses in all elements of IFU are calculated and the structure of the flow inside is studied in detail for the absence or presence of wind at a velocity from 0 to 35 m/s blowing from 5 main directions (0°, 45°, 90°, 135°, 180°). Studies are also carried out on the effect of the weather shield shape, the presence of baffles under it, and the rack in the shaft on the hydraulic losses.

As a result, the main sources of energy losses are identified and recommendations for the design of inlet shafts of this type are provided.

Based on the experience gained, an IFU configuration is found that provides a reduction in hydraulic losses relative to the baseline variant by 15%. Changing the IFU design will save 2.67 kg or 3.42 m³ per hour for each engine.

At the same time, the obtained design has reserves for improvement due to streamlining the flow under the weather shield using baffles.

The work carried out should be continued in the direction of analyzing the work of the UFI de-icing system and ensuring its effective operation in the whole range of operating parameters.

Moreover, it is planned to validate simulation results by experimental data after the inlet device will be manufactured and tested.

ACKNOWLEDGEMENTS

This work was supported by the Russian Federation President's grant (project code MK-3168.2019.8).

REFERENCES

- Air inlet Filtration for GAS turbines, 2019. *Access mode:* <http://www.folter.ru/en/catalog/vozdushnye-filtry-folter-dlya-gazovyh-turbin/>.
- Department of Aircraft Engine Theory, 2019. *Access mode:* <http://tdla.ssau.ru>.
- Druzhba pipeline – Wikipedia, 2019. *Access mode:* https://en.wikipedia.org/wiki/Druzhba_pipeline.
- Gazprom, 2019. *Access mode:* <http://www.gazprom.ru/>.
- INNOVAES | Innovación en Asuntos Estratégicos, 2019. *Access mode:* innovaes.com.
- JSC "Kuznetsov", 2019. *Access mode:* <http://www.kuznetsov-motors.ru/en>.
- RTEH GTD NK-16ST Vse o transporte gaza, 2019. *Access mode:* <http://www.turbinist.ru/6830-rte-gtd-nk-16st.html>.
- Samara University, 2019. *Access mode:* <https://ssau.ru/english>.
- Supercomputer Center - Samara University, 2019. *Access mode:* <https://ssau.ru/it/supercomputer>.
- VolgaEnergoGaz, 2019. *Access mode:* <http://www.v-eg.ru/>.
- Zabelin, N.A., Lykov, A.V., Rassokhin, V.A., 2013. *Calculation of available heat power of smoke fumes of gasocompressor units of russia's united gas transmission system.* Nauchno-tekhnicheskie vedomosti Cankt-Peterburgskogo gosudarstvennogo politekhnicheskogo universiteta. 4-1(183): 136-144.